Paleofire reconstruction based on an ensemble-member strategy applied to sedimentary charcoal

Olivier Blarquez,[1,2] Martin P. Girardin,[3] Bérangère Leys,[4] Adam A. Ali,[5] Julie C. Aleman,[4,5] Yves Bergeron,[2] and Christopher Carcaillet[4]

Received 9 April 2013; revised 18 April 2013; accepted 24 April 2013; published 7 June 2013.

[1] Paleofire events obtained from the statistical treatment of sedimentary charcoal records rely on a number of assumptions and user's choices, increasing the uncertainty of reconstructio\ns. Among the assumptions made when analyzing charcoal series is the choice of a filtering method for raw Charcoal Accumulation Rate ($CHAR_{raw}$). As there is no ultimate $CHAR_{raw}$ filtering method, we propose an ensemble-member approach to reconstruct fire events. We modified the commonly used procedure by including a routine replicating the analysis of a charcoal record using custom smoothing parameters. Dates of robust fire events, uncertainties in fire-return intervals and fire frequencies are derived from members' distributions. An application of the method is used to quantify uncertainties due to data treatment in two $CHAR_{raw}$ sequences from two different biomes, subalpine and boreal. **Citation:** Blarquez, O., M. P. Girardin, B. Leys, A. A. Ali, J. C. Aleman, Y. Bergeron, and C. Carcaillet (2013), Paleofire reconstruction based on an ensemble-member strategy applied to sedimentary charcoal, *Geophys. Res. Lett.*, *40*, 2667–2672, doi:10.1002/grl.50504.

1. Introduction

[2] Sedimentary charcoal records have proven useful for identifying long-term trends in fire activity at local to global scales, studying interactions with vegetation [*Clark*, 1990; *Blarquez and Carcaillet*, 2010] and the role of biomass burning in the carbon cycle [*Clark et al*., 1996; *Bremond et al*., 2011], and understanding the linkages with climatic changes [*Whitlock et al*., 2007; *Marlon et al*., 2008; *Ali et al*., 2012; *Nelson et al*., 2012]. Information contained in sedimentary charcoal records may reflect three different components: (i) amount of biomass burned (i.e., long-term trends in Charcoal Accumulation Rate (CHAR) or "background" trends) [*Marlon et al*., 2006; *Higuera et al*., 2011], (ii) fire frequency [*Gavin et al*., 2006], and (iii) noise [*Carcaillet et al*., 2007]. In the last decade, improvements were made in the methods used to examining charcoal records and in the quality of fire reconstructions. Noteworthy is the reconstruction of fire events by decomposing charcoal records into noise that mirrors taphonomical and sampling effects, and high-frequency charcoal peaks that could be related to fire events [*Long et al*., 1998; *Carcaillet et al*., 2001b]. The use of sieved charcoal ($ø > 150\,\mu m$) has led to spatially precise fire event reconstructions [*Carcaillet et al*., 2001a; *Lynch et al*., 2004]. Additionally, the use of a locally defined threshold for charcoal peak detection instead of a "globally" defined one has improved peak detection for records with varying mean and variance [*Higuera et al*., 2008]. Despite the progresses in paleofire research, the underlying methods behind fire reconstructions from sedimentary charcoal records rely on a number of analytical parameters that are determined by user choices. Here we present an approach based on ensemble members, i.e., a set of fire events reconstructions based on different analysis parameters, without *a priori* parameter choices to obtain robust history. By minimizing user analytical choices, the method we propose extends the capabilities of fire event reconstruction methods for sites located in all biomes such as the Mediterranean, tropical, temperate, and boreal.

2. Methods and Data Analysis

[3] The analysis of sedimentary charcoal records is composed of four main analytical steps [*Higuera et al*., 2009]: (1) Charcoal records are decomposed into Charcoal Accumulation Rates (CHAR) using the sediment age ~ depth model to obtain charcoal values for equivalent time steps and volumes along sedimentary sequences [*Long et al*., 1998]. CHAR are typically calculated at the median temporal resolution interval; (2) CHAR (subsequently $CHAR_{raw}$) are filtered using diverse smoothing methods to model the background component ($CHAR_{back}$), which is subtracted from the $CHAR_{raw}$ to obtain the residual high-frequency $CHAR_{peak}$; (3) $CHAR_{peak}$ is decomposed into two subpopulations using a Gaussian mixture model, with the first part being related to noise in the $CHAR_{peak}$ population ($CHAR_{noise}$), while the second part could represents the occurrence of one or more local fire events [*Gavin et al*., 2006]. For simplification, the $CHAR_{peak}$ exceeding $CHAR_{noise}$ was noted $CHAR_{fire}$. Additionally, we used the term fire events to describe the particular events from the $CHAR_{fire}$ that could represent one or more fires occurring in the surroundings of the lakes (< 1 km distance) [*Higuera et al*., 2007]. A given percentile of the $CHAR_{noise}$ is commonly used as a threshold to separate the $CHAR_{fire}$ from the $CHAR_{noise}$. The signal-to-noise index (SNI) is used to evaluate the effectiveness of the discrimination [*Kelly*

Additional supporting information may be found in the online version of this article.

[1]Université du Québec à Montréal, Montréal, Québec, Canada.
[2]Université du Québec en Abitibi-Témiscamingue, Rouyn-Noranda, Québec, Canada.
[3]Natural Resources Canada, Quebec City, Quebec, Canada.
[4]Ecole pratique des hautes études, Paris, France.
[5]Université Montpellier 2, Montpellier, France.

Corresponding author: O. Blarquez, Université du Québec en Abitibi-Témiscamingue, Rouyn-Noranda, Québec, Canada. (blarquez@gmail.com)

0094-8276/13/10.1002/grl.50504

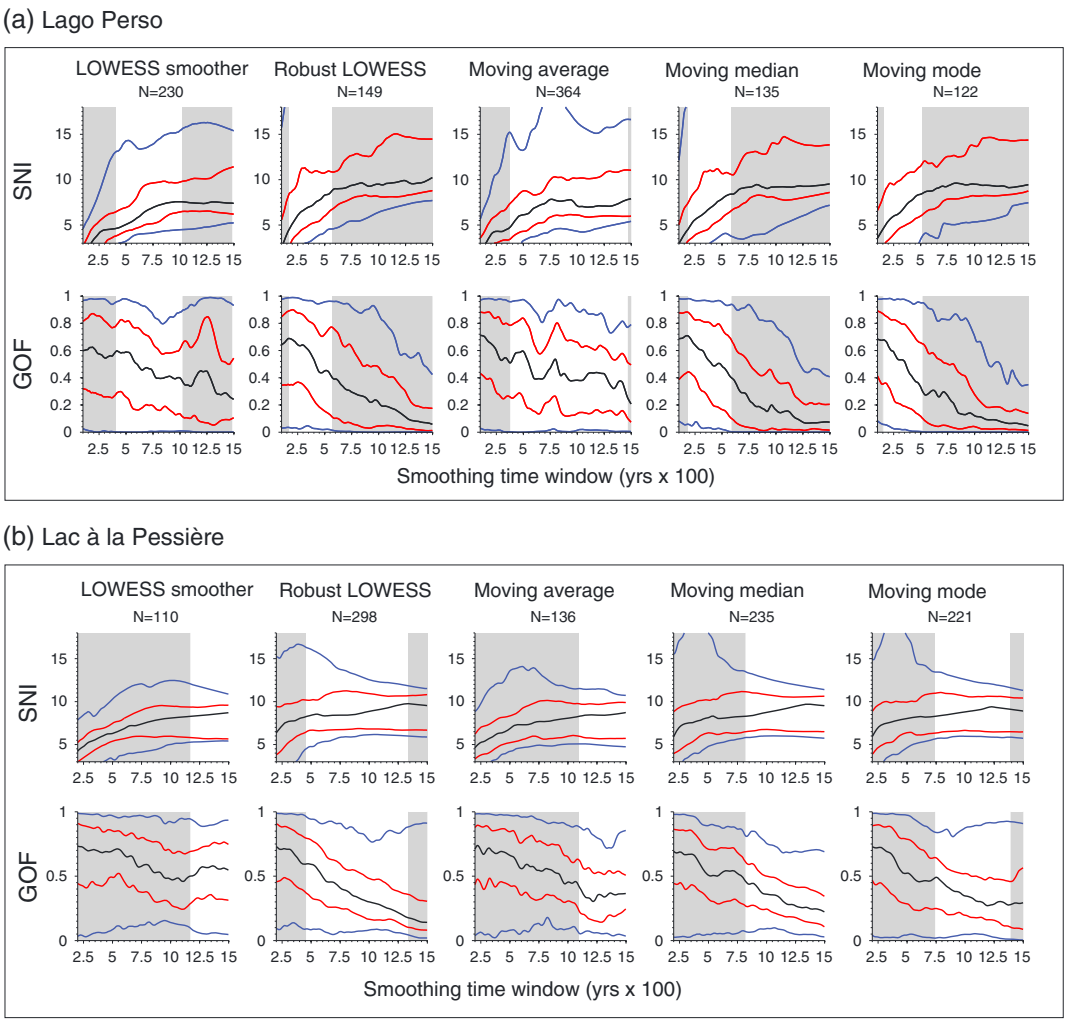

Figure 1. Signal to Noise Index (SNI) and Kolmogorov-Smirnov Goodness of Fit (GOF) *p*-values according to different filtering methods for the (a) Perso and (b) Pessière charcoal analyses plotted against moving window width. The filtering methods are the following: LOWESS, robust LOWESS, moving average, moving median, and moving mode filters, respectively. The median SNI and GOF are displayed using black lines, the red lines show 25th and 75th percentiles, respectively, and the blue lines show the 5th and 95th percentiles, respectively. The grey area shows the members rejected during the analysis, and the reconstruction number left for each filtering method is also shown.

et al., 2011]. The goodness-of-fit (GOF) metric is used to assess peak detection quality (i.e., the degree of contrast between the $CHAR_{noise}$ and the $CHAR_{fire}$) by comparing the empirical $CHAR_{noise}$ component with the one derived from the Gaussian mixture model. Significance is represented by the *p*-value of a Kolmogorov-Smirnov test, where large *p* indicates that the Gaussian mixture model adequately models empirical $CHAR_{noise}$. (4) $CHAR_{fire}$ is used to reconstruct local fire-return intervals (FRI) and fire frequency (FF) trends.

[4] Within this analysis, the second step ($CHAR_{raw}$ filtering) is particularly prone to inducing bias due to user choice. There is no consensus in the literature about the most appropriate method for filtering the $CHAR_{raw}$ series: They may be filtered using moving mode, median, average, inverse Fourier transform, locally weighted scatterplot smoothing (LOWESS) smoother, or LOWESS corrected for outliers, etc. [*Higuera et al.*, 2009]. Additionally, these filters are applied using varying temporal windows (mostly ranging from circa 300 to 1000 years), and the choice is generally guided by maximizing the SNI and GOF metrics (for a review on filtering methods in recent papers: *Higuera et al.* [2010]). To address the issue of parameter choices, we modified the CharAnalysis software [*Higuera et al.*, 2009] to include a routine that replicates the analysis of a charcoal record using custom smoothing parameters. We used the five chief available smoothing procedures: Moving Mode (MMo), Moving Median (MM), Moving Average (MA), LOWESS (LOWESS), and robust LOWESS (rLOWESS) filters, and for each procedure, we ran 470 analyses using various smoothing windows *t*, where $t = 100, 103, \ldots, 1501$. In total, an ensemble member of 2350 (470×5) fire event reconstructions is produced for each sedimentary charcoal record. As in the original procedure, the SNI and GOF are used as a selection criterion for fire event reconstructions. Given that the focus of this study was to test the effect of different filtering methods, we always calculated the $CHAR_{peak}$ component as a residual series (i.e., $CHAR_{peak} = CHAR_{raw} - CHAR_{back}$), and we used a locally defined threshold to

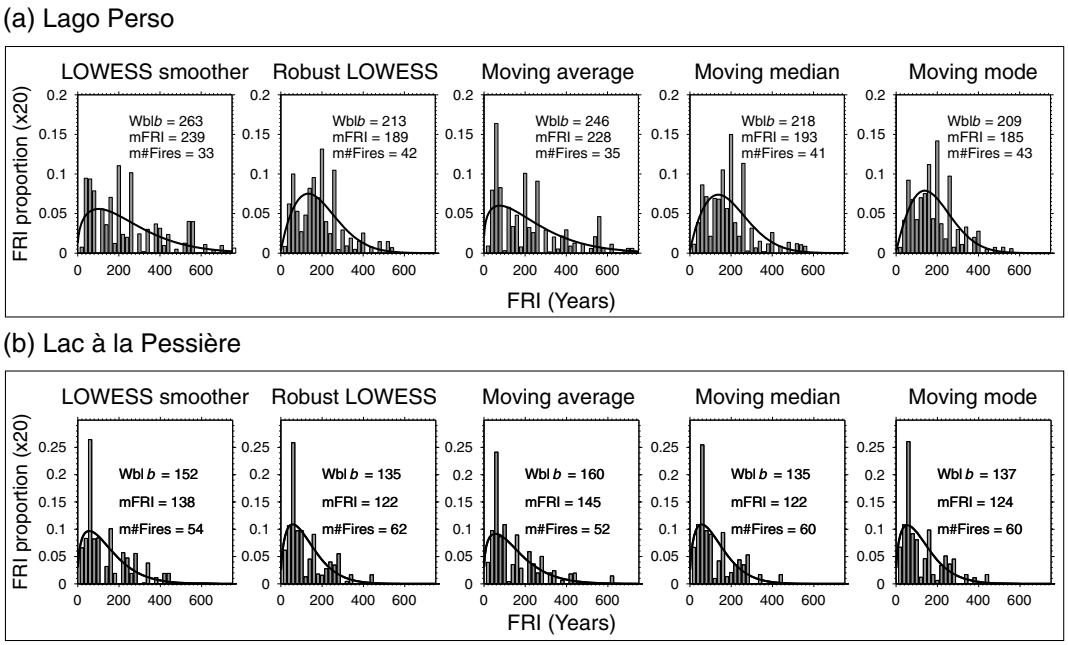

Figure 2. FRI distribution following the different filtering methods for (a) Perso and (b) Pessière charcoal records. FRI distribution associated with each filtering method (grey histogram). Each subfigure provides the fitted Weibull distributions (black line) and the associated Weibull *b* parameters (Wbl *b*), the mean number of fire events recorded (m#Fires) and the mean FRI by filtering method (mFRI).

separate the $CHAR_{noise}$ and $CHAR_{fire}$ components. These two procedures protect from biases related to variation in both the mean and variance of the empirical and simulated charcoal series [*Higuera et al*., 2010]. We did not screen peaks based on the original counts of charcoal peaks [see *Higuera et al*., 2009], because this procedure is specific to charcoal count data only [*Ali et al*., 2009]. At the final stage, the FRI distributions are modeled including the median FRI value, the mean number of reconstructed fire events and the Weibull *b* parameter that is estimated from the FRI distributions for each filtering method. For each reconstruction member fire date, a kernel density function [*Mudelsee et al*., 2004] is used to calculate FF. The median FF and percentiles of the reconstruction ensemble are estimated based on the distribution of all reconstruction members.

[5] For the studies requiring precise dating of fire events, we recommend that reconstructions should be guided by a consensus. Therein, within each reconstruction the number of fire events are determined and compared with the number of reconstructions identifying events for each time unit. The 75th percentile of this distribution is computed and selected as a threshold for defining the minimal number of members showing a fire by time unit, for a date being considered as a Robust Fire Event (RFE). This procedure eliminates fire dates related to analytical treatment and bias.

[6] To demonstrate our procedure, we applied it on sedimentary charcoal records from the subalpine Lago Perso (hereafter "Perso," 44°54′21″N 6°47′50″E) located at 2000 m above sea level (asl) within the municipality of Cesana Torinese, in the Susa Valley (Italy), and the boreal Lac à la Pessière (hereafter "Pessière," 49°30′30″N 79°14′25″W) located at 280 m asl in the black spruce forest of Quebec (Canada). The Perso and Pessière charcoal records spans the last 7900 and 7600 years, respectively. Charcoals were obtained using standard laboratory methods [*Carcaillet et al*., 2001b] and reported as areas ($mm^2\ cm^{-3}$). $CHAR_{raw}$ was calculated using median temporal resolution intervals, i.e., 14 and 13 years for Perso and Pessière. The Perso and Pessière records were chosen for their high-temporal resolution, the small lake areas (0.4 and 4.5 ha, respectively), and watersheds (0.27 km^2 at Perso and, unestimated at Pessière because the area is flat). The statistical properties of $CHAR_{raw}$ series required for peak analysis were satisfied in both cases [*Carcaillet et al*., 2001b; *Blarquez et al*., 2010]. For a complete description of the sites, see *Carcaillet et al*. [2001b] and *Blarquez et al*. [2010]. Codes and procedures presented in this paper are available as supporting information and online at http://blarquez.com/page/Codes/.

3. Results

3.1. Fire-event Reconstructions

[7] We applied the ensemble-member approach to the Perso and Pessière $CHAR_{raw}$ sequences to produce 2350 reconstructions. The member selection involved first excluding the members that have a GOF first quartile < 0.1 and thus showing a poorly modeled $CHAR_{noise}$. Within the resulting members the 1000 first showing the highest SNI were selected to produce the final ensemble member (corresponding to 43% of the initial members).

[8] Figure 1 illustrates the SNI and GOF distributions for the Perso and Pessière charcoal analyses. Smoothing windows ≥ 200 years gave a generally high SNI value for the Perso record (Figure 1a). This window size corresponds approximately to a width of 15 charcoal samples, which is below to the theoretical recommended 30-sample width for accurate peak detection [*Higuera et al*., 2009]. For the Pessière charcoal record, this sample size was generally

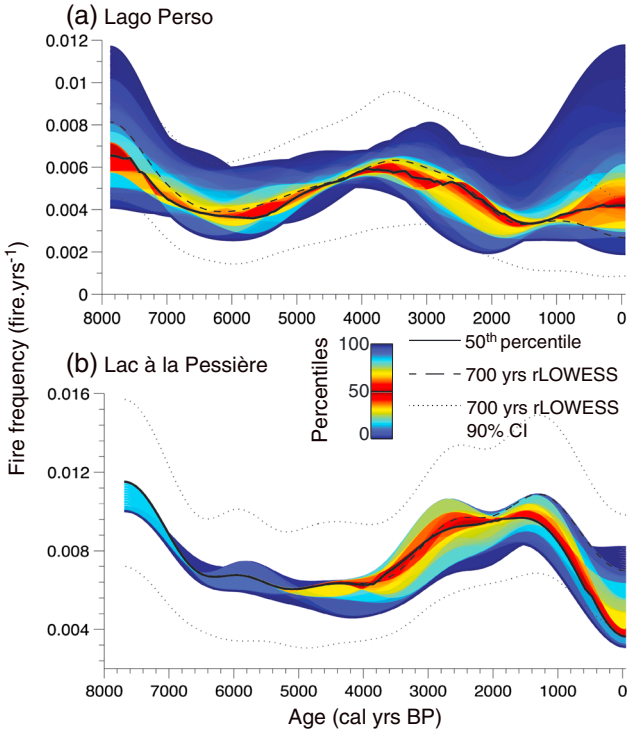

Figure 3. Fire frequency reconstructions of ensembles at (a) Perso and (b) Pessière. The black line corresponds to the median fire frequency (50th percentile) for the 1000 members at Perso and Pessière, respectively; percentiles of the reconstruction ensembles are shown using colors from red to blue (dark blue area encloses 100% of the members). Dashed black lines correspond to fire frequencies obtained with a filtering of the $CHAR_{raw}$ using a rLOWESS with a 700 year window width (the bootstrapped 90% confidence intervals are displayed using dashed lines).

not sufficient for accurate peak detection; an optimal window width was at least 57 to 76 samples (corresponding to circa 750 to 1000 years depending on the filtering method, Figure 1b). The GOF distribution is marked by the occurrence of low scores indicating that the Gaussian mixture model sometimes fails to accurately model the $CHAR_{noise}$ population, notably for the rLOWESS, MM, and MMo filters at Perso (Figure 1a). Based on the GOF criterion, the excluded reconstructions concerned window widths superior to 500 to 1000 years (Figures 1a and 1b). The rLOWESS, MM, and MMo filtering method appeared particularly prone to induce a poor distinction between $CHAR_{fire}$ and $CHAR_{noise}$ populations at Perso (only 149, 135, and 122 reconstructions left, respectively). Contrary, at Pessière, the lower number of reconstruction left is from the LOWESS and MA filtering methods (110 and 136 reconstructions).

[9] The RFE for each lake ensemble member analysis are shown in Figure S1 in the auxiliary material. From the Perso ensemble members, we were able to determine 33 fire events shared by the majority of the members (RFE) and not emerging from analytical bias (Figure S1a). At Pessière, 45 RFE were determined from the members' analysis (Figure S1b).

3.2. Variations Within the Reconstructed Fire Events

[10] Figure 2 shows FRI distributions by filtering method for the members shown in Figure 1, minus the excluded reconstructions (section 3.1). For both Perso and Pessière reconstruction members, we observed that, on average, the rLOWESS, MM, and MMo filters detected more events compared with the LOWESS and MA methods. For Perso, the rLOWESS, MM, and MMo filters gave similar mean FRIs of 189, 193, and 185 years, respectively ($p > 0.05$, Wilcoxon-Mann and Whitney *U*-test, Figure 2a). The situation is similar at Pessière, where the maximum event numbers were recorded using the rLOWESS, MMo, and MM filters (respectively, 62, 60, and 60 fires on average, with 122, 122, and 124 years associated mean FRIs, Figure 2b), while lower fire numbers were detected for the MA and LOWESS filters (52 and 54 fires on average, with 145 and 138 years associated mean FRIs, Figure 2b).

3.3. Reconstructing Fire Frequency (FF) History

[11] Fire frequency (FF) is treated here as the median of the ensemble-members FFs (Figure 3). When the ensemble FF is compared with the FF obtained with a single analysis of the Perso charcoal record (rLOWESS with a 700 year bandwidth), we noted only slight differences until circa 1000 cal yr B.P.; after this date, the two reconstructions diverged, with the rLOWESS reconstruction giving a lower fire frequency (Figure 3a). The Pessière ensemble-member median FF was similar to the FF obtained from the 700 years rLOWESS up to circa 2000 cal yr B.P.; after this date, the two reconstructions diverged, with the rLOWESS reconstruction at the upper limits of the ensemble-member reconstructions (Figure 3b). The uncertainty around the ensemble-member median for Perso is two times lower compared with the rLOWESS 90% confidence intervals (CI), until 2000 cal yr B.P. (i.e., a mean departure of 0.0025 fire yr^{-1} for the ensemble member 5th to 95th percentiles (90% CI), compared with 0.0055 fire yr^{-1} for the bootstrapped 90% CI). After 2000 cal yr B.P., ensemble-members uncertainty increase up to 0.0033 fire yr^{-1} (a value close to the 0.0042 fire yr^{-1} mean departure for the bootstrapped 90% CI). Uncertainty is more defined for the ensemble-member reconstruction from Pessière, where FF are highly conservative between 8000 and 4000 cal yr B.P., resulting in even lower ensemble-member percentile departures (i.e., a departure of 0.0020 fire yr^{-1} for the ensemble members, compared with 0.0067 fire yr^{-1} for the bootstrapped 90% CI).

4. Discussion

[12] Uncertainties related to user analytical choices may lead to different fire event reconstructions, even if the primary assumptions of statistical accuracy are met during the analysis process, i.e., good differentiation of charcoal peaks (high SNI values) and adequate modeling of $CHAR_{noise}$ (high GOF values). A single fire frequency history reconstruction related to an ultimate statistical treatment does not exist. We aim to select quality fire event reconstructions from a pool of members based on rational criteria (SNI and GOF). A consensus may be determined using the ensemble-member approach, which shows a fixed degree of statistical accuracy, from which fire history may be reconstructed. By diminishing the influence of user analytical choice, the main trends in data are highlighted (Figure 3).

[13] While the aim of most paleofire studies is to analyze general trends in frequency, some approaches require precisely dated fire events. This is the case when the goal is to analyze the effect or response of several variables (e.g.,

climate, land-use, and vegetation) following fire events using, for instance, superposed epoch analysis [*Blarquez and Carcaillet*, 2010] or when the goal is to calibrate the sedimentary charcoal signal using trapped charcoal [*Clark et al*., 1998] and fire scars [*Higuera et al*., 2011]. We showed here that robust fire events (RFE, Figure S1) could be determined using fire dates from the ensemble members. Fire events that are detected across all filtering methods and window widths, therefore, could be related to major events likely to have profoundly impacted ecosystems. The analysis of an event proxy and its response variable (e.g., in dendrochronology) is generally preceded by a sensitivity analysis aimed at finding a given event (e.g., fire) recorded by the majority of individuals taken from a sampled population (e.g., fire scars) [*Dieterich and Swetnam*, 1984], or to detect these significant events by comparison with a control population (e.g., detecting insect outbreaks) [*Speer et al*., 2001]. Sedimentary charcoal analysis generally lacks such control populations: when archives are available in the form of actual fires (from textual archives or dendrochronological series), the comparison between actual fires and fires assessed from sedimentary charcoal is usually limited to a few decades or centuries. While the ensemble member could be considered a population from which significant events can be found, overall sedimentary charcoal analysis will always benefit from calibration or verification using independent data.

[14] Paleofire assessments generally yield a unique set of possible fire dates, from which confidence intervals (CI) can be calculated by random resampling of these dates. The ensemble-member percentiles are not based on the probability that a detected fire actually occurred but on the detection probability of fires. If fire events are present in all members, then the associated fire frequency CI should diminish (e.g., Pessière record from 8000 to 4000 cal yr B.P., Figures 3b). In contrast, large variability in fire event detection should result in larger CI. Our approach should not only permit users to more accurately model fire frequency but also make it possible to assess CI directly related to fire event detection and thus the variability extant within charcoal record analysis. These new strategies have been successfully applied for two sedimentary charcoal sequences from the subalpine and the boreal biomes, indicating that they could be generalized to other biomes. We caution, however, that despite these statistical improvements, there are situations in which these analyses of sedimentary charcoal records are not recommended. Notably, results may be ecologically inaccurate if they are applied to a system where charcoal peaks tend to be small, or where the sedimentation rate is slow, and therefore, peaks are difficult to distinguish from background trends. Analyses proposed here should only be applied to robust charcoal records, i.e., with high enough sample sizes, good chronology, little sediment mixing, small lakes with a strong local source and small watersheds, not much sediment focusing and, a $CHAR_{peak}$ described by a mixture of two Gaussian distributions with different means and variances [*Gavin et al*., 2006].

[15] **Acknowledgments.** Financial support was provided by the Forest Complexity Modelling program (CRSNG-NSERC, Canada) to OB, the Canadian Forest Service to MPG, the FIREMAN program (ANR/ERA-net BiodivERsA) to CC, the NSERC of Canada to YB and AAA, the FRQNT to YB, and by grants from the École Pratique des Hautes Etudes to JA and BL and, from the Centre d'étude de la forêt to CC. The research was carried out within the framework of the International Associated Laboratory (LIA France-Canada) CNRS-UM2-EPHE-UQAT-UQAM-UQAC entitled MONTABOR: Forêts montagnardes et boréales: chrono-écologie et aménagement écosystémique durable.

[16] The Editor thanks two anonymous reviewers for their assistance in evaluating this paper.

References

Ali, A. A., P. E. Higuera, Y. Bergeron, and C. Carcaillet (2009), Comparing fire-history interpretations based on area, number and estimated volume of macroscopic charcoal in lake sediments, *Quatern. Res.*, *72*, 462–468.

Ali, A. A., et al. (2012), Control of the multi-millennial wildfire size in boreal North America by spring climatic conditions, *Proc. Natl. Acad. Sci. USA*, *109*(51), 20775–20776.

Blarquez, O., and C. Carcaillet (2010), Fire, fuel composition and resilience threshold in subalpine ecosystem, *PLoS One*, *5*(8), e12480.

Blarquez, O., L. Bremond, and C. Carcaillet (2010), Holocene fires and a herb-dominated understorey track wetter climates in subalpine forests, *J. Ecol.*, *98*(6), 1358–1368.

Bremond, L., C. Carcaillet, C. Favier, A. A. Ali, C. Paitre, Y. Bégin, Y. Bergeron, and P. J. H. Richard (2011), Effects of vegetation zones and climatic changes on fire-induced atmospheric carbon emissions: A model based on paleodata, *Int. J. Wildland Fire*, *19*(8), 1015–1025.

Carcaillet, C., M. Bouvier, B. Fréchette, A. C. Larouche, and P. J. H. Richard (2001a), Comparison of pollen-slide and sieving methods in lacustrine charcoal analyses for local and regional fire history, *Holocene*, *11*, 467–476.

Carcaillet, C., Y. Bergeron, P. J. H. Richard, B. Frechette, S. Gauthier, and Y. T. Prairie (2001b), Change of fire frequency in the eastern Canadian boreal forests during the Holocene: Does vegetation composition or climate trigger the fire regime?, *J. Ecol.*, *89*(6), 930–946.

Carcaillet, C., A.-S. Perroux, A. Genries, and Y. Perrette (2007), Sedimentary charcoal pattern in a karstic underground lake, Vercors massif, French Alps: Implications for palaeo-fire history, *Holocene*, *17*(6), 845–850.

Clark, J. S. (1990), Fire and climate change during the last 750 yr in Northwestern Minnesota, *Ecol. Monogr.*, *60*(2), 135–159.

Clark, J. S., B. J. Stocks, and P. J. H. Richard (1996), Climate implications of biomass burning since the 19th century in eastern North America, *Global Change Biol.*, *2*(5), 433–442.

Clark, J. S., J. Lynch, B. J. Stocks, and J. G. Goldammer (1998), Relationships between charcoal particles in air and sediments in west-central Siberia, *Holocene*, *8*(1), 19–29.

Dieterich, J. H., and T. W. Swetnam (1984), Dendrochronology of a fire-scarred ponderosa pine, *For. Sci.*, *30*(1), 238–247.

Gavin, D. G., F. S. Hu, K. Lertzman, and P. Corbett (2006), Weak climatic control of stand-scale fire history during the late Holocene, *Ecology*, *87*(7), 1722–1732.

Higuera, P. E., M. E. Peters, L. B. Brubaker, and D. G. Gavin (2007), Understanding the origin and analysis of sediment-charcoal records with a simulation model, *Quaternary Sci. Rev.*, *26*(13–14), 1790–1809.

Higuera, P. E., L. B. Brubaker, P. M. Anderson, T. A. Brown, A. T. Kennedy, and F. S. Hu (2008), Frequent fires in ancient shrub tundra: Implications of paleorecords for arctic environmental change, *PLoS One*, *3*(3), e0001744.

Higuera, P. E., L. B. Brubaker, P. M. Anderson, F. S. Hu, and T. A. Brown (2009), Vegetation mediated the impacts of postglacial climate change on fire regimes in the south-central Brooks Range, Alaska, *Ecol. Monogr.*, *79*(2), 201–219.

Higuera, P. E., D. G. Gavin, P. J. Bartlein, and D. J. Hallett (2010), Peak detection in sediment–charcoal records: Impacts of alternative data analysis methods on fire-history interpretations, *Int. J. Wildland Fire*, *19*(8), 996–1014.

Higuera, P. E., C. Whitlock, and J. A. Gage (2011), Linking tree-ring and sediment-charcoal records to reconstruct fire occurrence and area burned in subalpine forests of Yellowstone National Park, USA, *Holocene*, *21*(2), 327–341.

Kelly, R. F., P. E. Higuera, C. M. Barrett, and F. S. Hu (2011), A signal-to-noise index to quantify the potential for peak detection in sediment–charcoal records, *Quatern. Res.*, *75*(1), 11–17.

Long, C. J., C. Whitlock, P. J. Bartlein, and S. H. Millspaugh (1998), A 9000-year fire history from the Oregon Coast Range, based on a high-resolution charcoal study, *Can. J. For. Res.*, *28*(5), 774–787.

Lynch, J. A., J. S. Clark, and B. J. Stocks (2004), Charcoal production, dispersal, and deposition from the Fort Providence experimental fire: Interpreting fire regimes from charcoal records in boreal forests, *Can. J. For. Res.*, *34*(8), 1642–1656.

Marlon, J., P. J. Bartlein, and C. Whitlock (2006), Fire-fuel-climate linkages in the northwestern USA during the Holocene, *Holocene*, *16*(8), 1059–1071.

Marlon, J. R., J. P. Bartlein, C. Carcaillet, D. G. Gavin, S. P. Harrison, P. E. Higuera, F. Joos, M. J. Power, and I. C. Prentice (2008), Climate and human influences on global biomass burning over the past two millennia, *Nature Geosci.*, *1*, 697–702.

Mudelsee, M., M. Börngen, G. Tetzlaff, and U. Grünewald (2004), Extreme floods in central Europe over the past 500 years: Role of cyclone pathway "Zugstrasse Vb", *J. Geophys. Res.*, *109*(D23), D23101.

Nelson, D. M., D. Verschuren, M. A. Urban, and F. S. Hu (2012), Long-term variability and rainfall control of savanna fire regimes in equatorial East Africa, *Global Change Biol.*, *18*(10), 3169–3170.

Speer, J. H., T. W. Swetnam, B. E. Wickman, and A. Youngblood (2001), Changes in pandora moth outbreak dynamics during the past 622 years, *Ecology*, *82*(3), 679–697.

Whitlock, C., P. I. Moreno, and P. Bartlein (2007), Climatic controls of Holocene fire patterns in southern South America, *Quatern. Res.*, *68*(1), 28–36.